Color and Glossiness Reproduction of 3D Object Surface

Hideaki Haneishi, Takuya Iwanami, Tomoyuki Honma, Norimichi Tsumura and Yoichi Miyake
Department of Information and Image Sciences, Chiba University
Chiba, Japan

Abstract

The method proposed for extracting goniospectral information of 3D objects is reformulated in more exact form. Especially the illumination direction is expressed in both azimuthal and elevation angle. It is shown that extending the range of illumination direction to two dimension leads to provide useful model parameters including the surface normal of the object. Experimental results of the display simulation are also presented to demonstrate the visual effect of changing the light source distribution.

Introduction

In the electronic museum or the internet shopping, reproducing the color and glossiness of 3D object with high fidelity is desired for observers or consumers to recognize more exactly how the object is. Spectral information is necessary for exact representation of color objects and many researchers have made efforts to obtain it[1-5]. However, any paper does not address the extraction of the characteristics necessary to reproduce the glossiness of the object.

For the reflection analysis of the inhomogeneous dielectric objects, the dichromatic reflection model is usually used in which the reflection on the object is composed of the diffuse reflection (body reflection) and the surface reflection (specular reflection)[6]. Perception of glossiness is basically induced by the specular reflection on the object surface. Sato and Ikeuchi have proposed a method to extract the glossiness of a 3D object[7]. They acquired a sequence of images by changing the position of light source while keeping the object and camera fixed. They have shown that from the analysis of the sequence of images, the goniophotometric property can be extracted at each pixel in the image locally. However, their technique treats only three-band image (RGB) which is not sufficient for recovering the spectral information.

In a previous paper[8], we have proposed a method for obtaining gonio-spectral information of the object, which has been developed independently of Sato and Ikeuchi but

was found to be an extended version of their method. As shown in Fig. 1, light sources are located at several different positions while 3D objects and the viewing position are fixed. Multiband images are taken under the illumination from each light source. The images are then analyzed and the parameters representing goniospectral characteristics of the object are extracted and archived.

Once such information is obtained, we can estimate the spectral distribution at any point of not-occluded surface of the object under an arbitrary spectral and spatial distribution of light source. In consequence, we can display its tristimulus values on a calibrated color CRT. Observers or consumers may enjoy the appearance of the object under a variety of light sources and then recognize the object's intrinsic color and surface characteristics more exactly.
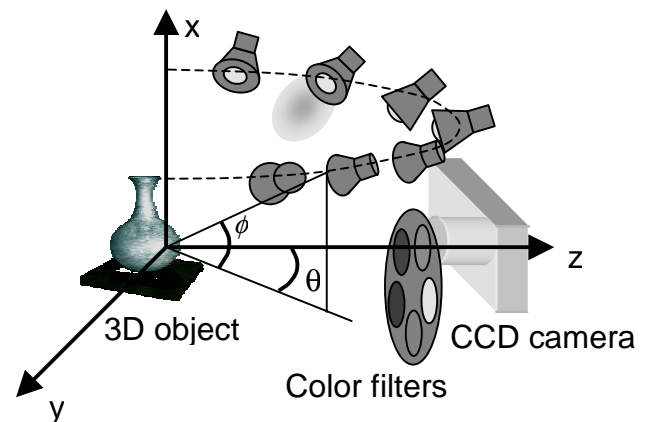

Figure 1. Multi-angle illuminant, multi-band imaging system.

In this paper, we generalize the formulation of the imaging system and reflection model so as to express the geometry of multi-angle illuminant, multi-band-imaging system exactly. Here the variation of the illumination direction is extended to two dimensions (azimuthal and elevation angle), which allows the extraction of the reflection model parameters related to the object shape. Experimental results using practical objects are also presented.

Dichromatic Reflection Model

In this section, we first formulate a physical model of spectral light reflection on the object. Next we show what factors are required for the display simulation of objects under an arbitrary distribution of light source.

The coordinate system used in this paper is shown in Fig. 1. Now we denote spectral power distribution at position $\mathbf{r}$ on the object surface by a column vector $\mathbf{f}(\mathbf{r};\theta,\phi)$ when illuminated from the direction of azimuthal angle θ and elevation angle ϕ. According to the dichromatic reflection model it is denoted as a synthesis of the surface-reflection component, $\mathbf{f}_s$, and the diffuse-reflection component, $\mathbf{f}_d$:

$$\mathbf{f}(\mathbf{r};\theta,\phi) = \mathbf{f}_s(\mathbf{r};\theta,\phi) + \mathbf{f}_d(\mathbf{r};\theta,\phi) \quad (1)$$

We further assume that each term can be represented as

$$\mathbf{f}_s(\mathbf{r};\theta,\phi) = w_s(\mathbf{r};\theta,\phi)\mathbf{Lo}_w \quad (2a)$$

$$\mathbf{f}_d(\mathbf{r};\theta,\phi) = w_d(\mathbf{r};\theta,\phi)\mathbf{Lo}(\mathbf{r}) \quad (2b)$$

Here $w_s(\mathbf{r};\theta,\phi)$, $w_d(\mathbf{r};\theta,\phi)$ denote a geometry-dependent factor of specular and diffuse light, respectively. $\mathbf{L}$ is a diagonal matrix whose diagonal elements represent the spectral radiance of the illuminant. $\mathbf{o}(\mathbf{r})$ denotes a column vector of spectral reflectance of the object. On the other hand, $\mathbf{o}_w$ denotes a column vector whose elements are a common constant, accordingly $\mathbf{Lo}_w$ represents spectral radiance proportional to illuminant. Thus the equation (2a) means that the specular component is the same as the illuminant spectra in vector orientation.

Each term of Eq. (1) is written by a product of the normalized vector and the magnitude.

$$\mathbf{f}(\mathbf{r};\theta,\phi) = w_s^{(n)}(\mathbf{r};\theta,\phi)\mathbf{e}_s + w_d^{(n)}(\mathbf{r};\theta,\phi)\mathbf{e}_d(\mathbf{r}) \quad (3)$$

where

$$\mathbf{e}_s = \frac{\mathbf{Lo}_w}{\|\mathbf{Lo}_w\|} \quad (4a)$$

$$\mathbf{e}_d(\mathbf{r}) = \frac{\mathbf{Lo}(\mathbf{r})}{\|\mathbf{Lo}(\mathbf{r})\|} \quad (4b)$$

$$w_s^{(n)}(\mathbf{r};\theta,\phi) = w_s(\mathbf{r};\theta,\phi)\|\mathbf{Lo}_w\| \quad (4c)$$

$$w_d^{(n)}(\mathbf{r};\theta,\phi) = w_d(\mathbf{r};\theta,\phi)\|\mathbf{Lo}(\mathbf{r})\| \quad (4d)$$

What we want to know here are four factors listed above, namely (1) the unit vector $\mathbf{e}_s$ which gives the spectral direction of the specular component and does not depend on the position $\mathbf{r}$, (2) the unit vector $\mathbf{e}_d(\mathbf{r})$ which gives the spectral direction of diffuse component, (3) two scalar functions, $w_s^{(n)}(\mathbf{r};\theta,\phi)$ and $w_d^{(n)}(\mathbf{r};\theta,\phi)$ which both depend on the geometry of the object surface and illumination angle. If these vectors and functions are obtained independently, one can simulate the appearance of the object under an arbitrary spectral distribution of light source with arbitrary illumination angle by the following steps; 1) eliminating the illuminant used for image acquisition by multiplying the inverse of $\mathbf{L}$ by two unit vectors, 2) applying the illuminant for display simulation $\mathbf{L}'$, 3) multiplying the geometrical factor of each component at the new illumination angle (θ',ϕ'). These operations are expressed by the following equations:

$$w_s^{(n)}(\mathbf{r},\theta',\phi')\mathbf{L}'\mathbf{L}^{-1}\mathbf{e}_s = w_s(\mathbf{r},\theta',\phi')\mathbf{L}'\mathbf{o}_w \quad (5a)$$

$$w_d^{(n)}(\mathbf{r},\theta',\phi')\mathbf{L}'\mathbf{L}^{-1}\mathbf{e}_d(\mathbf{r}) = w_d(\mathbf{r},\theta',\phi')\mathbf{L}'\mathbf{o}(\mathbf{r}) \quad (5b)$$

Finally by synthesizing these two components, the object under such illumination can be simulated as

$$\hat{\mathbf{f}}(\mathbf{r};\theta',\phi',\mathbf{L}') = w_s(\mathbf{r};\theta',\phi')\mathbf{L}'\mathbf{o}_w + w_d(\mathbf{r};\theta',\phi')\mathbf{L}'\mathbf{o}(\mathbf{r}) \quad (6)$$

More generally, arbitrary spatial distribution of the light source, e. g., a long fluorescent lamp, can be simulated as,

$$\hat{\mathbf{f}}(\mathbf{r};\mathbf{L}'(\theta',\phi')) = \iint \{w_s(\mathbf{r};\theta',\phi')\mathbf{L}'(\theta',\phi')\mathbf{o}_w$$
$$+ w_d(\mathbf{r};\theta',\phi')\mathbf{L}'(\theta',\phi')\mathbf{o}(\mathbf{r})\}d\theta'd\phi' \quad (7)$$

Here $\mathbf{L}'(\theta',\phi')$ represents the spectral distribution of illuminant at the angle (θ',ϕ'). In the next section, we show how to estimate these four factors.

Method for Display Simulation

Multiband Image Acquisition System

Theoretically two unit vectors, $\mathbf{e}_s$, $\mathbf{e}_d$ have a high dimensionality and two geometrical factors $w_s^{(n)}$, $w_d^{(n)}$ are the functions of two continuous variables, θ,ϕ. However, it is not practical to capture many narrow-band images of the object under each of densely spaced light sources. Instead, we use sparsely located light sources with respect to spatial sampling, and we use a limited number of spectral bands with respect to spectral sampling. From such limited information, w estimate the gonio-spectral property under a light source with arbitrary illumination angle and spectral distribution, based on the assumption that both characteristics possess smooth variation.

Light sources of imaging system are placed at several (N) different positions so as to cover the range of illumination angle expected in display simulation. Each of light sources illuminates a 3D object by turn and its multiband images are captured by a CCD camera with five color filters. The appropriate number of filters depends on the statistical distribution of spectra of the target objects. Based on our experience of measuring the reflectance spectra of 147 oil paint color patches[3], we empirically decided to use five bands.

We denote the spectral radiance of the object under ith light source with the illumination angle of ($\theta^{(i)},\phi^{(i)}$) as

$$\mathbf{f}(\mathbf{r};\theta^{(i)},\phi^{(i)}) = \mathbf{f}_s(\mathbf{r};\theta^{(i)},\phi^{(i)}) + \mathbf{f}_d(\mathbf{r};\theta^{(i)},\phi^{(i)})$$
$$= w_s(\mathbf{r};\theta^{(i)},\phi^{(i)})\mathbf{Lo}_w + w_d(\mathbf{r};\theta^{(i)},\phi^{(i)})\mathbf{Lo}(\mathbf{r}). \quad (8)$$

The pixel value of the multiband image for this spectral radiance is expressed as

$$\mathbf{g}(\mathbf{r};\theta^{(i)},\phi^{(i)}) = \mathbf{Hf}(\mathbf{r};\theta^{(i)},\phi^{(i)})$$
$$= w_s(\mathbf{r};\theta^{(i)},\phi^{(i)})\mathbf{HLo}_w + w_d(\mathbf{r};\theta^{(i)},\phi^{(i)})\mathbf{HLo(r)}$$
(9)

Here $\mathbf{H}$ denotes a system matrix whose row each represents overall spectral sensitivity of camera with the corresponding filter. Thus, this matrix transforms spectral radiance of light to multiband pixel values.

The above equation is also written by using normalized vectors as

$$\mathbf{g}(\mathbf{r};\theta^{(i)},\phi^{(i)}) = w_s^{(n)}(\mathbf{r};\theta^{(i)},\phi^{(i)})\mathbf{e}_s + w_d^{(n)}(\mathbf{r};\theta^{(i)},\phi^{(i)})\mathbf{e}_d(\mathbf{r}) \quad (10)$$

Here we redefine the unit vectors as

$$\mathbf{e}_s = \frac{\mathbf{HLo}_w}{\|\mathbf{HLo}_w\|} \tag{11a}$$

$$\mathbf{e}_d(\mathbf{r}) = \frac{\mathbf{HLo(r)}}{\|\mathbf{HLo(r)}\|} \tag{11b}$$

$$w_s^{(n)}(\mathbf{r};\theta^{(i)},\phi^{(i)}) = w_s(\mathbf{r};\theta^{(i)},\phi^{(i)})\|\mathbf{HLo}_w\| \tag{11c}$$

$$w_d^{(n)}(\mathbf{r};\theta^{(i)},\phi^{(i)}) = w_d(\mathbf{r};\theta^{(i)},\phi^{(i)})\|\mathbf{HLo(r)}\| \tag{11d}$$

Unlike the case of Eqs. (4) and (5), for the display simulation, the pseudo inverse of the matrix $\mathbf{H}$ must be multiplied by two unit vectors prior to applying $\mathbf{L}^{-1}$.

How to Estimate Gonio-spectral factors

Let us consider the behavior of pixel values at a certain pixel $\mathbf{r}$ in the multiband images obtained. We denote the array of pixel values by vectors $\{\mathbf{g}(\mathbf{r};\theta^{(i)},\phi^{(i)})\}_{i=1,...,N}$.
According to the dichromatic reflection model[6], these vectors approximately lie on a common plane spanned by a vector of specular component and a vector of diffuse component as shown in Eq. (10). Using this property, we determine the two unit vectors, then calculate two geometrical functions.

(a) $\mathbf{e}_s$

We have used a reference white object (BaSO$_4$ plate) since its spectral reflectance is approximated by $\mathbf{o}_w$. By imaging it together with the target object and extracting its multiband pixel values, the direction of illuminant spectrum can be estimated. Putting a white object is possible under our well-controlled imaging condition, unlike the general condition in computer vision. However, a more sophisticated method which does not require any reference white object may be used to simplify the preparation of image[9].

(b) $\mathbf{e}_d(\mathbf{r})$

If the illumination angle in the imaging system is varied widely enough, it is expected that there exists at least one illumination angle at which the light from the object excludes the specular component almost completely. In the multiband vector space, such vector should make its angle from the specular component maximum. Thus, if one finds such a vector and normalize it as Eq. (12), it would be a unit vector of diffuse component.

$$\mathbf{e}_d(\mathbf{r}) \equiv \{\mathbf{g}(\mathbf{r};\theta^{(i)},\phi^{(i)})/\|\mathbf{g}(\mathbf{r};\theta^{(i)},\phi^{(i)})\| | i = \arg\max_j \phi_j\} \quad (12)$$

Practically, however, the vector array has variation from the plane more or less due to noise, system's instability,

non-linearity, etc. Therefore we first determine the plane which best fits the vector array by the least square method, then project each vector onto the plane. After that, the vector that gives the maximum angle from the specular component is found and $\mathbf{e}_d(\mathbf{r})$ is calculated.

(c) Geometrical factors, $w_s^{(n)}(\mathbf{r};\theta^{(i)},\phi^{(i)})$, $w_d^{(n)}(\mathbf{r};\theta^{(i)},\phi^{(i)})$

Once unit vectors, $\mathbf{e}_s$ and $\mathbf{e}_d(\mathbf{r})$ become known, two scalars, $w_s^{(n)}(\mathbf{r};\theta^{(i)},\phi^{(i)})$, $w_d^{(n)}(\mathbf{r};\theta^{(i)},\phi^{(i)})$ are obtained by solving Eq. (10).

Pseudo-inverse of Matrix H

In this study, we determine the inverse matrix $\mathbf{H}^-$ by a regression analysis using a set of color patches. The spectral radiance of each patch under the illuminant used for image acquisition is measured by a spectroradiometer, while the corresponding pixel values of multiband image are recorded by the multiband camera. Then, the inverse matrix $\mathbf{H}^-$ is given by

$$\mathbf{H}^- = \mathbf{FG}^T(\mathbf{GG}^T)^{-1} \tag{13}$$

where $\mathbf{F}$ is a matrix whose column is the spectral radiance of each color patch while $\mathbf{G}$ is a matrix whose column is multiband pixel values of each color patch. $\mathbf{FG}^T$, $\mathbf{GG}^T$ represents the correlation matrix between $\mathbf{f}$ and $\mathbf{g}$, the auto-correlation matrix of $\mathbf{g}$, respectively[10]. In our experiment we used 24 color patches of the Macbeth color checker.

Approximation of Gonio-photometric Factor by Using Phong Model

As described before, we need continuos functions, $w_d^{(n)}(\mathbf{r};\theta,\phi)$, $w_s^{(n)}(\mathbf{r};\theta,\phi)$ rather than the discrete data set $w_d^{(n)}(\mathbf{r};\theta^{(i)},\phi^{(i)})$, $w_s^{(n)}(\mathbf{r};\theta^{(i)},\phi^{(i)})$. We modeled these components on the basis of Phong model[11] as

$$\hat{w}_s^{(n)}(\mathbf{r},\theta,\phi) = A_s(\mathbf{r})\cos^{\alpha(\mathbf{r})}(\theta-\theta_s(\mathbf{r}))\cos^{\alpha(\mathbf{r})}(\phi-\phi_s(\mathbf{r})) \quad (14)$$

$$\hat{w}_d^{(n)}(\mathbf{r};\theta,\phi) = A_d(\mathbf{r})\cos(\theta-\theta_d(\mathbf{r}))\cos(\phi-\phi_d(\mathbf{r})) \tag{15}$$

$A_s(\mathbf{r})$, $\theta_s(\mathbf{r})$, $\phi_s(\mathbf{r})$, $\alpha(\mathbf{r})$, $A_d(\mathbf{r})$, $\theta_d(\mathbf{r})$, $\phi_d(\mathbf{r})$ are the model parameters and determined so that the approximated values best fit to the data set $w_s^{(n)}(\mathbf{r};\theta^{(i)},\phi^{(i)})$ and $w_d^{(n)}(\mathbf{r};\theta^{(i)},\phi^{(i)})$. MATLAB optimization toolbox was used for this fitting. Note that we assumed in this mode that there is no angular dependency in diffuse and specular reflection.

Procedure of Image Display Simulation

We summarize a procedure of image display simulation below.

(1) Multiply the pseudo-inverse, $\mathbf{H}^-$ by the specular and diffuse unit vector, respectively.

(2) Multiply the inverse matrix $\mathbf{L}^{-1}$ by both components to remove the effect of illuminant for image acquisition.

(3) Multiply the new illuminant $\mathbf{L}'$ by both components.

(4) Multiply the geometrical factors, w_s and w_d by the corresponding component, respectively.

(5) If spatially broad light sources are simulated, repeat (1)-(4) for each light source position and calculate the summation.

(6) Multiply the color matching functions of the calibrated CRT for display.

$$\mathbf{v}(\mathbf{r}, \mathbf{L}'(\theta', \phi'))$$

$$= \mathbf{T} \int w_s^{(n)}(\mathbf{r}, \theta', \phi') \mathbf{L}'(\theta', \phi') \mathbf{L}^{-1} \mathbf{H}^- \cdot \frac{\mathbf{HLo}_w}{\|\mathbf{HLo}_w\|} d\theta' d\phi' \qquad (16)$$

$$+ \mathbf{T} \int w_d^{(n)}(\mathbf{r}, \theta', \phi') \mathbf{L}'(\theta', \phi') \mathbf{L}^{-1} \mathbf{H}^- \cdot \frac{\mathbf{HLo}(\mathbf{r})}{\|\mathbf{HLo}(\mathbf{r})\|} d\theta' d\phi'$$

$\mathbf{T}$ is a matrix whose rows are the color matching functions. Receiving this RGB signals, a well-calibrated CRT may produce tristimulus values same as the color of the object under the virtual illuminant.

If we take into account the effect on the ambient light when watching the CRT, we must implement further any color appearance model into the above procedure [12]. Such task is beyond the scope of this paper. Note that our goal here is to reproduce the physical tristimulus values of the object under the virtual illuminant.

Experiment

Multiband-image acquisition experiments were conducted using of some dielectric objects including a colored styrofoam sphere and a china bottle. The five band-pass filters used in the image acquisition have the following center wavelength (FWHM in nm), 420(55), 450(60), 500(55), 550(55), 600(70)nm. A cooled monochromatic CCD camera (MUTOH, CV04) with 16bit quantization levels and 384x256 pixel resolution was used. The distance between the light sources and the object was about 1.8m.

In the experiment, we prepared two kinds of arrangement of light sources:

(1) Seven azimuthal angles θ =-45,-30,-15,0,15,30,45 in degree were used while elevation angle ϕ was fixed at about 12 degree. In this case, Eqs. (14),(15) are written as

$$\hat{w}_s^{(n)}(\mathbf{r}, \theta, \phi) = A_s'(\mathbf{r}) \cos^{\alpha(\mathbf{r})}(\theta - \theta_s(\mathbf{r})) \qquad (17)$$

$$\hat{w}_d^{(n)}(\mathbf{r}; \theta, \phi) = A_d'(\mathbf{r}) \cos(\theta - \theta_d(\mathbf{r})) \qquad (18)$$

where

$$A_s'(\mathbf{r}) = A_s(\mathbf{r}) \cos^{\alpha(\mathbf{r})}(\phi - \phi_s(\mathbf{r}))$$

$$A_d'(\mathbf{r}) = A_d(\mathbf{r}) \cos(\phi - \phi_d(\mathbf{r})) .$$

Note that only As' and Ad' are estimated and that the individual parameters, A_s, ϕ_s, A_d, and ϕ_d are not estimated separately. Thus, the display simulation is possible only for the fixed elevation angle, $\phi = 12$.

(2) Seven azimuthal angles θ =-45,-30,-15,0,15,30,45 at a fixed elevation angle ($\phi = 12$) and seven elevation angles $\phi = 0,6,12,18,24,36$ at an fixed azimuthal angle ($\theta = 15$) were used. In this case, we can potentially estimate all the parameters of Eqs. (14) and (15).

Geometrical Parameter Estimation

Using the second arrangement of the light source, we estimated the model parameters of the sphere object. Figure 2 shows an example of the intensity of diffuse component at a certain point as a function of azimuthal and elevation angle. Fitting by cosine functions are successful for both angles. On the other hand, fitting of specular components was not easy. Specular component has usually has a spiky curve. The sparse sampling sometimes is unstable in extracting the model parameters.
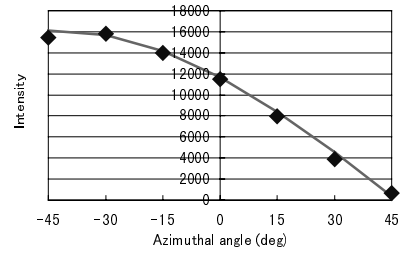

Figure 2. Intensity of diffuse component vs. illumination angle.

Assuming the Lambertian model for the diffuse component, the model parameters $\theta_d(\mathbf{r})$ and $\phi_d(\mathbf{r})$ give the normal of the object surface at the position $\mathbf{r}$. In fact, we could estimate the shape of the spherical object from these parameters in some degree. Figure 3 shows the result. Except for the marginal area, the spherical shape is estimated successfully. This result suggests that this information may be used to support the model parameter estimation of specular components.
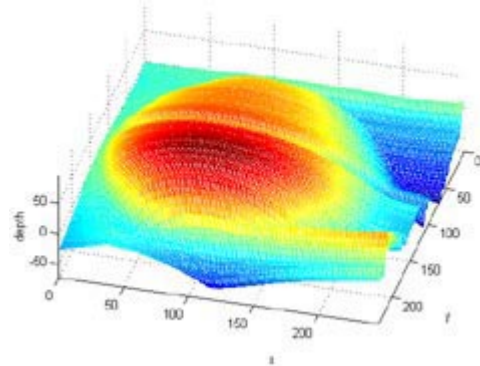

Figure 3. 3D shape of spherical object reconstructed from the model parameters θ_d and ϕ_d.

Display Simulation and GUI-based Display Tool

We show the display simulation by the light source array of case (1). Figure 4 shows examples of china bottle image; (a) under tungsten lamp (3150K) at θ =45 degree. (b) under daylight type light source (5900K) with spatially broad extension(θ =45 - 135 degree). Seeing both images may help to understand the glossiness and color on the object surface more exactly than seeing either one image.
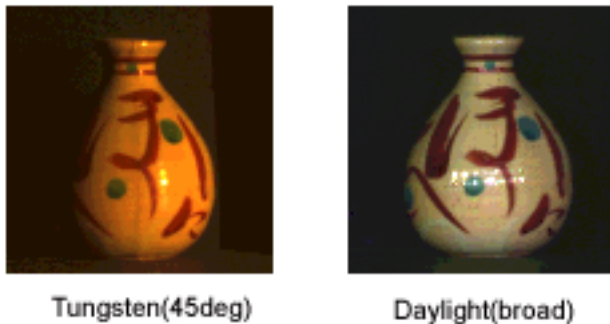

Tungsten(45deg)   Daylight(broad)

Figure 4. Display simulation of a china bottle.

We built a prototype of GUI-based display tool for display simulation using MATLAB. This software allows the simulation of moving light source. Figure 5 shows the GUI window. User first chooses the illuminant color from the buttons, and determine the range of the light source movement by entering the start and stop angles. It was confirmed that animation image has potential to allow observers to recognize the shape and surface property of 3D objects. Quick and smooth display of animation image is still under study.
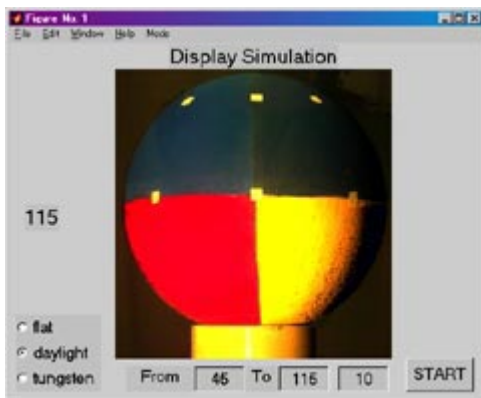

Figure 5. GUI window for display simulation.

Conclusion

The method proposed for extracting goniospectral information of 3D objects was reformulated in more exact form. Especially the geometry of illumination angle was expressed in azimuthal and elevation angle. Extending the range of illumination direction to two dimension (θ and ϕ) allows a wider variety of light sources. Such an extension of illumination direction also have a potential in estimating the model parameters related to the object shape. This information may be used for the model parameter related to the specular components. Experimental results of the display simulation have been also presented to demonstrate the visual effect of changing the light source distribution.

Acknowledgement

References

1. K. Martinez, J. Cupitt, D. Saunders, High resolution color imaging of paintings, *Proc. SPIE* **1901**, 25-36 (1993)
2. H. Maitre, F. J. M. Schmitt, J. -P. Crettez, Y. Wu, J. Y. Hardeberg, Spectrophotometric image analysis of fine art paintings, *Proc. IS&T/SID fourth Color Imaging Conference*, 50-53 (1996)
3. H. Haneishi, T. Hasegawa, N. Tsumura and Y. Miyake, Design of color filters for recording artworks, *IS&T's 50th Annual Conference*, Boston, 369-372 (1997)
4. F. Konig, Reconstruction of natural spectra from color sensor using nonlinear estimation method, *Proc. IS&T's 50th Annual Conference*, Boston, 454-458 (1997)
5. F. H. Imai and R. S. Berns, High-resolution multi-spectral image archives: A hybrid approach, *Proc. IS&T/SID sixth Color Imaging Conference*, 224-227 (1998)
6. S. Shafer, Using color to separate reflection components, *Color Res. and appl.*, 10(4), 210-218 (1985)
7. Y. Sato and K. Ikeuchi, Reflectance analysis for 3D computer graphics model generation, *Graph. Mod. and Im. Proc.,* **58**(5), 437-451 (1996)
8. H. Haneishi, T. Iwanami, T. Honma, N. Tsumura and Y. Miyake, Goniospectral imaging of 3D objects, *IS&T/SID's 6th Color Imaging Conference*, Scottsdale, 173-176 (1998)
9. S. Tominaga, Multichannel vision system for estimating surface and illumination functions, *J. Opt. Soc. Amer.*, **13**, 2163-2173 (1996)
10. W. K. Pratt, *Digital Image Processing*, *2nd Edition*, Wiley Interscience, New York (1991)
11. Phong Bui-Tuong, Illumination for computer generated pictures, *Communications of the ACM*, **18**, 311-317 (1975)
12. K. M. Braun, M. D. Fairchild, Testing five color-appearance models for changing in viewing conditions, *Color Res. and Appl.*, **22**,165-173 (1997).